Improvement of a Transmission Rate for a Multiple-Input Single-Output Visible Light Communication System

Aki Kaizu, Masataka Imao and Satoko Miki
Advanced Technology R&D Center
Mitsubishi Electric Corporation
Kyoto, JAPAN

***Abstract*—Visible light communication (VLC) has attracted much attention with the growth of a light emitting diode (LED). An LED has ability to blink at high speed compared to a fluorescent lamp. Therefore, we consider a multiple-input single-output (MISO) VLC system using multiple LEDs. However, signal distortion caused by a limited frequency response of LED drive circuits leads a bottleneck in transmission rate improvement. Hence in this paper, we propose a novel demodulation method based on the Viterbi algorithm. The proposed method has high performance in robustness against signal distortion, and provides 80% improvement in a transmission rate compared to the conventional method.**

I. Introduction

Visible light communication (VLC) is optical wireless communication that carries data by modulated light in the spectrum of visible light. The visible light is principally used for illumination. Furthermore, interest in VLC has grown rapidly with the growth of light emitting diodes (LEDs). An LED has ability to blink at high speed compared to a fluorescent lamp. Hence, VLC has attracted attention as an area of research [1]-[5] and standardization [6]. Therefore, we develop a multiple-input single-output (MISO) VLC system with applying practical LEDs for the purpose of transmitting large-sized data.

In our development system, information data is modulated using on-off keying (OOK) which is the most simple modulation method, and the data is transmitted from several LEDs on a transmitter. These LEDs can transmit each different data for the purpose of improvement in a transmission rate. A receiver obtains modulated light using a photo diode (PD), and demodulates received data by applying the Viterbi algorithm [7].

An improvement in a transmission rate can be achieved by applying short OOK symbol. However, an LED drive circuit generally has a limited frequency response compared to that of a PD. Furthermore, an LED drive circuit may have low performance in a frequency response. The reason is that a practical LED is not designed to be required to blink at a high rate. Therefore, signal distortion caused by a frequency response of an LED drive circuit leads a bottleneck in transmission rate improvement.

Hence in this paper, a novel demodulation method based on the Viterbi algorithm is proposed. The proposed method has high performance in robustness against signal distortion, and enables to accelerate a transmission rate in case of using an LED drive circuit with a limited frequency response. In order to reveal the performance of our proposed method, simulation results are shown.

This paper is organized as follows. In sections II and III, the system model and the Viterbi algorithm equipped in the receiver are described. Then the issue in a frequency response of LED drive circuits and a problem of a conventional method are discussed in section IV. In section V, the novel demodulation method based on the Viterbi algorithm is shown. Simulation results are shown in section VI. Finally, conclusions are given in section VII.

II. System Model

A. *Overview of System Model*

VLC has a merit that LED illumination can be used as a part of a transmitter. Moreover, the transmitter can send data to a specific area since visible light has sharp directivity compared to radio wave.

One of the applications that take advantage of VLC characteristics is an indoor positioning system [8], [9]. A receiver of this system obtains positional data from illumination arranged in the indoor ceiling. In this case, transmission of the positional data can be performed by a low rate of several kilobits per second. On the other hand, a system for transmitting large-sized data such as video signal requires a high transmission rate. Therefore, in this paper, transmission rate improvement for VLC is discussed. In addition, the system uses LEDs having practical drive circuit design and components since drive circuits of common LED are not arranged for a high transmission rate.

First, Fig. 1 shows a system image of VLC. This system is composed of a transmitter and a receiver. The transmitter contains illumination device on a ceiling, and its device has several sockets of a straight tube type LED. The receiver is arranged in a position which is covered with illuminating light.

Next, Fig. 2 shows a block diagram of our VLC system. This system is a MISO system.

The transmitter is composed of a control unit and several LED drive circuits containing a straight tube type LED. Each straight tube type LED transmits different data to accelerate a transmission rate. In this paper, we assume that the number of straight tube type LEDs is two because of simplification of this system.

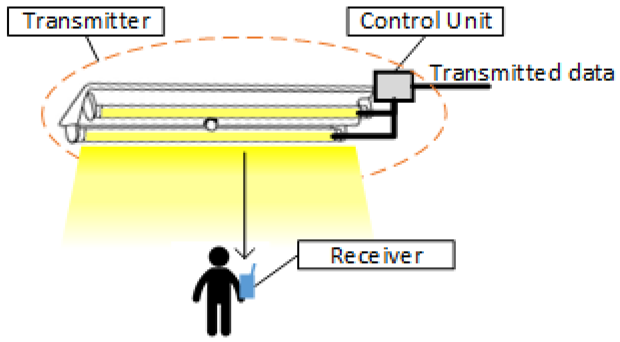

Fig. 1. A system image of VLC.

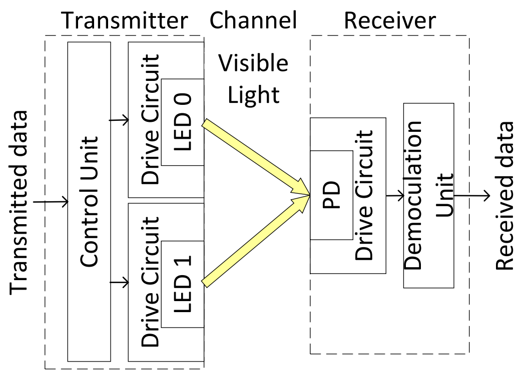

Fig. 2. A block diagram of our VLC system.

The receiver is composed of a demodulation unit, a PD and its drive circuit. The number of PDs in this system is one so that the receiver can be downsized.

B. Transmitter

Fig. 3 shows a block diagram of the transmitter. The transmitter is composed of a control unit, two straight tube type LEDs and its LED drive circuits. The control unit is composed of an S/P (Serial-to-Parallel) conversion block, OOK blocks and timing delay block.

First, the transmitted data is divided into two parallel data sets at the S/P conversion block. These data sets are defined as $x_{even} = (x_k \mid k \text{ is even.})$ and $x_{odd} = (x_k \mid k \text{ is odd.})$, respectively, where x_k is a k th transmitted data bit.

Next, the OOK blocks modulate x_{even} and x_{odd} using OOK. The output signals $y_0(t)$ and $y_1(t)$ are expressed by

$$\begin{cases} y_0(t) = x_k \left(k \text{ is even.}, \dfrac{k}{2} T_s < t \le \left(\dfrac{k}{2} + 1 \right) T_s \right) \\ y_1(t) = x_k \left(k \text{ is odd.}, \dfrac{k-1}{2} T_s < t \le \left(\dfrac{k-1}{2} + 1 \right) T_s \right), \end{cases} \tag{1}$$

where T_s is an OOK symbol length. Note that OOK symbols $y_0(t)$ and $y_1(t)$ are synchronized.

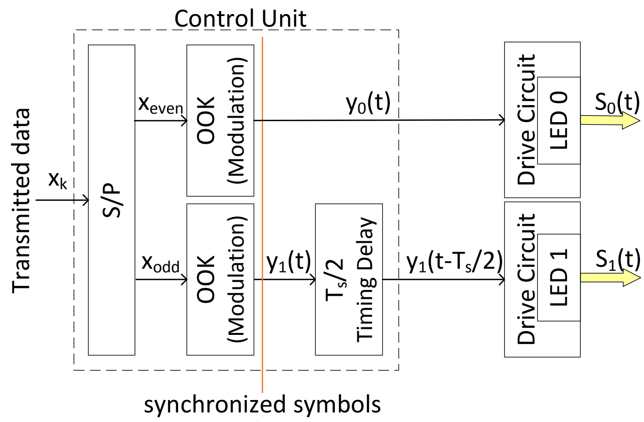

Fig. 3. A block diagram of the transmitter.

The timing delay block delays $y_1(t)$ referring time delay of d , and outputs $y_1(t-d)$ to the drive circuit of LED1. Notice that, d is given by the following equation.

$$d = \frac{1}{2} T_s . \tag{2}$$

The receiver can distinguish between signals transmitted from LED0 and LED1 by performing its timing delay process.

Finally, the i th LED outputs light using an LED drive circuit. Luminance $s_i(t)$ of LED0 and LED1 are proportional to $y_0(t)$ and $y_1(t-d)$, respectively.

C. Received Signal Modeling

A received signal $r(t)$ is defined as

$$r(t) = \sum_{i=0}^{1} w_i s_i(t) + n, \tag{3}$$

where w_i is channel gain that is determined by aperture area of a PD or a distance between a PD and i th LED [10]. Though n is a summation of thermal and shot noise, n can be defined as Gaussian noise in case of receiving of adequate light. Hence we suppose that the PD receives strong light in this paper.

On the other hand, a distance between the PD and the each LED has almost the same since all LEDs are arranged in a same illumination device. Therefore we assume that w_0 and w_1 should be considered as equal.Then $r(t)$ can be written by

$$r(t) = w \sum_{i=0}^{1} s_i(t) + n \quad (w = w_0 = w_1). \tag{4}$$

Fig. 4 shows the examples of waveform of $s_0(t)$, $s_1(t)$ and $r(t)$. In this figure, k th symbol means an OOK symbol corresponding to x_k . The received signal $r(t)$ has three amplitude levels. Therefore the receiver needs to equip amplitude demodulator.

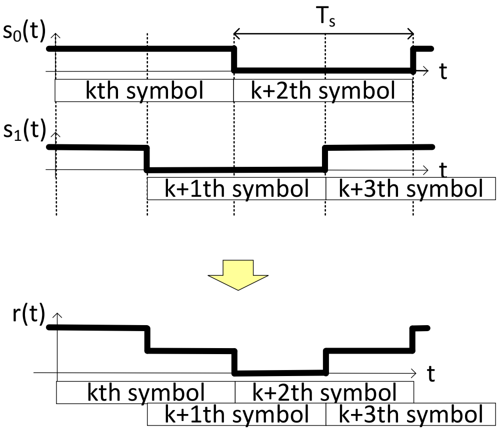

Fig. 4. The transmitted signals and the received signal.

D. Receiver

Fig. 5 shows a block diagram of the receiver. The receiver is composed of a demodulation unit, a PD and its drive circuit. The demodulation unit is composed of a signal integration block and a Viterbi algorithm block.

First, the PD detects intensity of modulated light, and a PD drive circuit converts its intensity to an electrical received signal $r(t)$.

Next, The signal integration block integrates $r(t)$, and calculates a sample a_k including information of $k-1$ th, k th and $k+1$ th transmitted data. The sample a_k is expressed by

$$a_k = \int_{-Ts/4}^{Ts/4} r\left(t_k + \frac{T_s}{2} + t\right) dt, \tag{5}$$

where t_k is the time of k th symbol head. Fig. 6 shows the integration range of $r(t)$ for calculating of a_k.

Next, the Viterbi algorithm block applies the Viterbi algorithm to the sample sequence $a_k, a_{k+1}, \ldots$. The Viterbi algorithm is a decode method that obtains maximum likelihood sequence with a small calculation amount. Therefore its block outputs a received data sequence $\hat{x}_k, \hat{x}_{k+1}, \ldots$ of maximum likelihood.

III. VITERBI ALGORITHM

In this section, the method of signal estimation applying the Viterbi algorithm is described. This method outputs calculation result based on a branch metric and structure of a trellis diagram. Fig. 7 shows a trellis diagram corresponding to the sample sequence $a_k, a_{k+1}, \ldots$.

A branch metric is defined by the negative log-likelihood [11]. Hence, in case of considering only Gaussian noise, a branch metric $B(z_{k-1}z_k \to z_k z_{k+1})$ for a branch connecting state $z_{k-1}z_k$ to state $z_k z_{k+1}$ is defined as

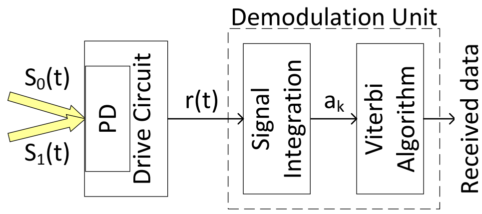

Fig. 5. A block diagram of the receiver.

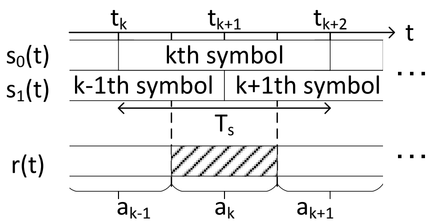

Fig. 6. Integration range of the received signal.

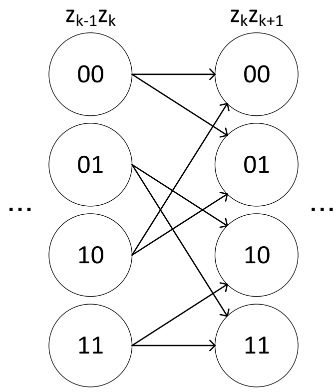

Fig. 7. A trellis diagram for the Viterbi algorithm.

$$\begin{aligned} & B(z_{k-1}z_k \to z_k z_{k+1}) \\ &= -\ln\left(p\left(a_k \middle| x_{k-1} = z_{k-1}, x_k = z_k, x_{k+1} = z_{k+1}\right)\right) \\ &= C\left(a_k - \right. \\ & \qquad \left. ave\left(a_k \middle| x_{k-1} = z_{k-1}, x_k = z_k, x_{k+1} = z_{k+1}\right)\right)^2, \end{aligned} \tag{6}$$

where $p(a_k \mid X)$, $ave(a_k \mid X)$ and C are the conditional probability of a_k given X, the conditional average of a_k given X, and constant value corresponding to variance of Gaussian noise n, respectively. $ave(a_k \mid x_{k-1}, x_k, x_{k+1})$ is given by the following equation.

$$\begin{aligned} & ave(a_k \mid x_{k-1}, x_k, x_{k+1}) \\ &= x_k \frac{T_s}{2} + (x_{k-1} + x_{k+1}) \frac{T_s}{4}. \end{aligned} \tag{7}$$

The channel gain w in $r(t)$ was assumed to be compensated by auto gain control (AGC).

Calculation result based on the above branch metric is obtained at the Viterbi algorithm. Therefore, a received data sequence $\hat{x}_k, \hat{x}_{k+1}, \ldots$ of maximum likelihood is obtained from the sample sequence $a_k, a_{k+1}, \ldots$.

IV. Frequency Response of an LED Drive Circuit

A. Overview of Frequency Response

An LED drive circuit has a frequency response. Therefore, the luminance $s_i(t)$ of i th LED has distortion caused by the frequency response in i th LED drive circuit. In case of long symbol length, its distortion becomes relatively small. However, in case of short symbol length for the purpose of improvement in a transmission rate, its distortion cannot be ignored.

A maximum likelihood sequence for the received signal affected by Gaussian noise is obtained by applying the Viterbi algorithm using the branch metric described in the previous section. However, distortion caused by the frequency response gives another signal deterioration and it causes degradation of demodulation performance. Therefore, a novel demodulation method that has high performance in robustness against signal distortion caused by the frequency response is necessary for achieving improvement in a transmission rate.

B. Influence of Frequency Response

In this subsection, we describe a detail of a frequency response in an LED drive circuit.

An LED needs a drive circuit to output light with intensity proportional to $y_i(t)$. Furthermore, the drive circuit has a frequency response depending on circuit characteristics. The LED drive circuit can be modeled as a RC low-pass filter [12].

In case of short symbol length for the purpose of improvement in a transmission rate, the high frequency components in $y_i(t)$ are increased. Therefore, distortion of the luminance $s_i(t)$ caused by a frequency response of low-pass filter is increased.

Considering distortion caused by the frequency response, $s_i(t)$ is replaced by following,

$$\hat{s}_i(t) = \frac{\tau}{\tau+\Delta t} s_i(t-\Delta t) + \left(1-\frac{\tau}{\tau+\Delta t}\right) y_i\left(t-\frac{i}{2}T_s\right), \tag{8}$$

where τ and Δt are a value depending on a cut-off frequency f and elapsed time from t, respectively. The relationship between τ and f is defined as following condition.

$$f = \frac{1}{2\pi\tau}. \tag{9}$$

V. Proposed Method

In this section, a novel demodulation method based on the Viterbi algorithm is proposed. The method has high performance in robustness against signal distortion.

A. Overview of Proposed Method

The branch metric of the conventional method is expressed with using the conditional probability of a_k given x_{k-1}, x_k and x_{k+1} in Eq. (6) since the sample a_k depends on 3 bits transmitted data of x_{k-1}, x_k and x_{k+1}.

On the other hand, in case of rising/falling edge of $y_i(t)$, high frequency components are increased and $\hat{s}_i(t)$ is distorted at symbol boundary. Therefore, the distortion occurs in the front region of an OOK symbol due to time delay characteristic of low-pass filter.

The sample a_k is composed of a rear region of the $k-1$th symbol, a central region of the k th symbol and a front region of the $k+1$th symbol in Fig. 6. Note that a front region of the $k+1$th symbol may contain much distortion. Therefore, we propose to calculate the branch metric without the $k+1$th transmitted data x_{k+1} related to the $k+1$th symbol containing much distortion.

Fig. 8 shows a trellis diagram of the proposed method. Suppose that the sample a_k is depended on 2 bit transmitted data of x_{k-1} and x_k. Received data based on the proposed branch metric and structure of the trellis diagram is obtained at the Viterbi algorithm block.

B. Proposed Branch Metric

In this subsection, a detail of the proposed branch metric is described.

The $k+1$th transmission data x_{k+1} is removed from a calculation condition of likelihood. Therefore, the proposed branch metric $B'(z_{k-1} \to z_k)$ for a branch connecting state z_{k-1} to state z_k is defined as

$$\begin{aligned} &B'(z_{k-1} \to z_k) \\ &= C'\left(a_k - ave\left(a_k \middle| x_{k-1} = z_{k-1}, x_k = z_k\right)\right)^2, \end{aligned} \tag{10}$$

where C' is constant value corresponding to the variance of Gaussian noise n. We suppose that the occurrence probability $p(x_{k+1})$ of x_{k+1} sets 1/2 so that calculation of $ave(a_k \mid x_{k-1}, x_k)$ becomes possible. Then $ave(a_k \mid x_{k-1}, x_k)$ is given by the following equation.

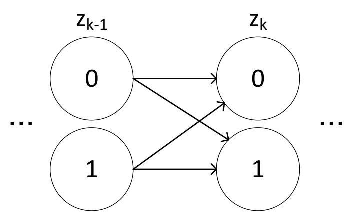

Fig. 8. A trellis diagram of the proposed method.

$$ave(a_k \mid x_{k-1}, x_k) = x_k \frac{T_s}{2} + \left(x_{k-1} + \frac{1}{2} \right) \frac{T_s}{4} \qquad (11)$$
$$\left(p(x_{k+1}) = 1/2 ,\ x_{k+1} = 0,1 \right).$$

The channel gain w in $r(t)$ was assumed to be compensated by AGC.

Received data based on the above proposed branch metric is obtained at the Viterbi algorithm block.

VI. Simulation and Discussion

In this section, the simulation results of the proposed method are shown. The transmitter and receiver in Fig. 3 and 5 are demonstrated in our computer simulation.

A. Simulation Condition

Table I shows parameters applied in the simulation. The transmitted data is random binary data, and the number of samples per OOK symbol is set as 16 in the transmitted and received signals. Cut-off frequency f in Eq. (9) is set as 1 MHz since its value can be realized by a practical circuit design and components for common illumination. Moreover, received signal is calculated from luminance using Eq. (4). Note that the channel gain w was assumed to be compensated by AGC. Furthermore, the Viterbi algorithm block in the receiver decodes received data by applying the procedure based on the Viterbi algorithm. The proposed method and the conventional method are described in section V and III, respectively.

In this simulation, Gaussian noise n assumes to be compensated by signal integration in the integration block to evaluate the robustness against signal distortion caused by a frequency response. Furthermore, the OOK symbol length varies depending on a transmission rate.

B. Received Signal

Figs. 9-11 show waveforms of the received signal $r(t)$ and an ideal received signal without distortion. The received signal is calculated from luminance using Eq. (4). The horizontal axis of these figures is time, and the vertical axis represents a value obtained by normalizing the received signal intensity. Figs. 9-11 show waveforms in transmission rates of 1 Mbps, 3 Mbps and 6 Mbps, respectively. These figures indicate that, in case of short symbol length and a high transmission rate, high frequency components that is contained in the ideal signal is increased. Therefore, the distortion of received signal is relatively increased.

C. BER

In case of ideal system, the received signal is not distorted and no received error is occurred even if a transmission rate is high. However, in case of the real system, received error is grown with increase of a transmission rate because of distortion of received signal.

We evaluate performances of the proposed method, the conventional method and the method without Viterbi algorithm. Fig. 12 shows the simulation result. The horizontal axis of the figure is a transmission rate, and the vertical axis

TABLE I. Simulation Parameters

The number of straight tube type LEDs	2
The number of PDs	1
Transmitted data	Random binary data
Samples/symbol	16
Cut-off frequency in an LED drive circuit	1 MHz

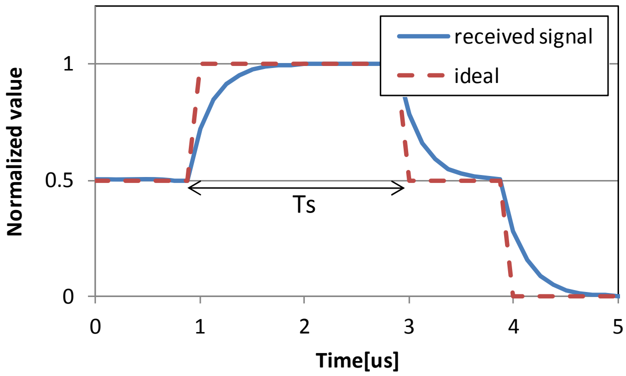

Fig. 9. The received signal of a transmission rate of 1 Mbps.

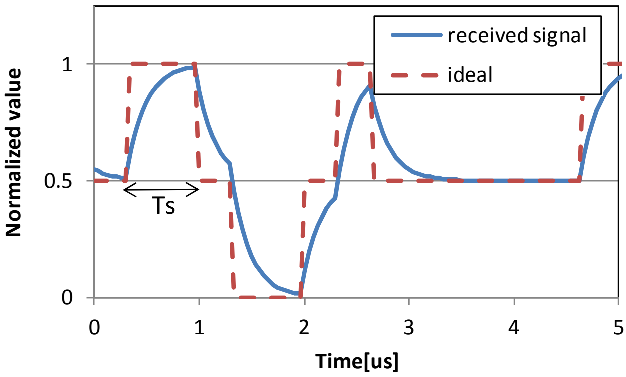

Fig. 10. The received signal of a transmission rate of 3 Mbps.

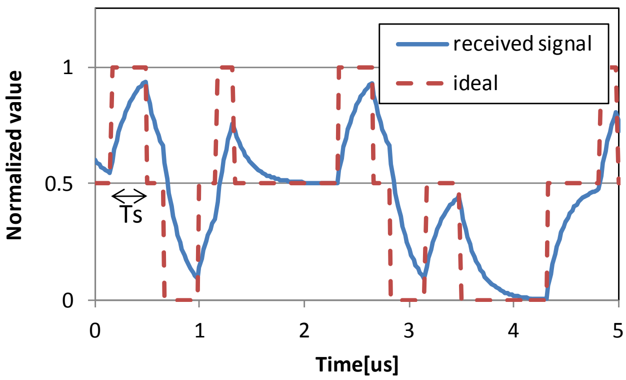

Fig. 11. The received signal of a transmission rate of 6 Mbps.

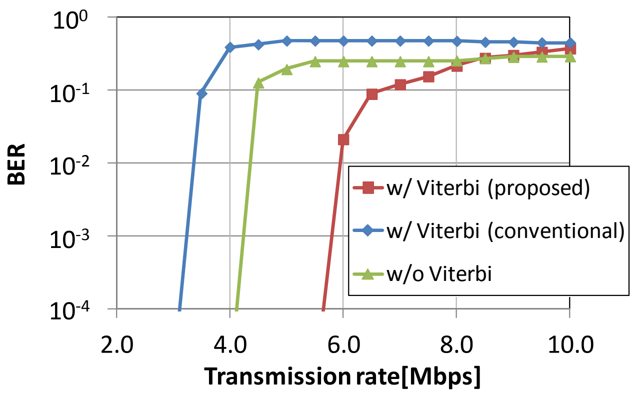

Fig. 12. BER vs a transmission rate.

represents a bit error rate (BER). Bit error is determined by comparing the transmitted data and the received data, and BER is expressed by

$$BER = ERROR\_NUM / TRANS\_NUM \,, \qquad (12)$$

where TRANS_NUM and ERROR_NUM are the total number of transmitted data bits and the total number of error bits, respectively.

In case of the method without Viterbi algorithm, a control unit of a transmitter only has an OOK block. Two LEDs on the transmitter output same light, and luminance of its LEDs is proportional to the output level of OOK block. A receiver of the method without Viterbi algorithm integrates the received signal samples over a symbol and performs OOK demodulation with decision threshold. In the method without Viterbi algorithm, samples per symbol and symbol length are set to 1/2 times of the other methods for fair comparison.

Fig. 12 reveals the proposed method enables improvement in a transmission rate compared to the other methods. A maximum transmission rate under the condition of BER of 10^{-4} is 3.0 Mbps in the conventional method, 4.5 Mbps in the method without Viterbi algorithm and 5.5 Mbps in the proposed method. The proposed method can achieve transmission rate improvement of 80% and 35% compared to the conventional method and the method without Viterbi algorithm.

The demodulator of the proposed method and conventional method needs to perform amplitude demodulation since the received signal has three amplitude levels. Therefore, the conventional method has less performance in robustness against signal distortion compared to the method without Viterbi algorithm.

On the other hand, symbol length of the proposed method is long compared to the method without Viterbi algorithm, and hence the proposed method can remove transmission data related to the symbol containing much distortion from calculation condition of likelihood. Therefore, the robustness against distortion caused by a frequency response was improved by applying the proposed method. Consequently the proposed method enables a high transmission rate compared to the other methods.

VII. Conclusion

In this paper, a novel demodulation method based on the Viterbi algorithm is proposed. The proposed method improves a transmission rate for a VLC system containing LED drive circuits with a limited frequency response. In the proposed method, we removed transmitted data related to the symbol containing much distortion from a calculation condition of likelihood so that the robustness against signal distortion caused by the frequency response is improved. The simulation result showed that the proposed method achieved 80% improvement in a transmission rate compared to the conventional method. The study of the influences of thermal noise, shot noise and strength change of received signal for mobile reception will be an area for further research.

References

[1] T. Komine and M. Nakagawa, "Fundamental analysis for visible light communications using LED lights," IEEE Trans. Consumer Electronics, vol.50, no.1, pp.100-107, Feb. 2004.

[2] K. Ebihara, K. Kamakura and T. Yamazato, "Layered space-time coding using LED array for image-sensor-based visible light communications," 2015 IEEE International Conference on Communications (ICC), London, pp.5048-5053, June 2015.

[3] Y. Wang, M. Zhang, Y. Wang, W. Fang, L. Tao and N. Chi, "Experimental demonstration of visible light communication based on sub-carrier multiplexing of Multiple-Input-Single-Output OFDM," Proc. 17th Opto-Electronics and Communications Conference, Busan, Korea, pp.745-746, July 2012.

[4] L. Zeng, D. O'Brien, H. Minh, G. Faulkner, K. Lee, D. Jung, Y. Oh and E. T. Won, "High data rate multiple input multiple output (MIMO) optical wireless communications using white LED lighting," IEEE J. Sel. Areas Commun., vol.27, no.9, pp.1654-1662, Dec. 2009.

[5] A. H. Azhar, T. Tran, D. O'Brien, "A Gigabit/s indoor wireless transmission using MIMO-OFDM visible-light communications," IEEE Photonics Technology Letters, vol.25, no.2, pp.171-174, Jan. 2013.

[6] Standard of Japan Electronics and Information Technology Industries Association, JEITA CP-1223, "Visible Light Beacon System," May 2013.

[7] A. J. Viterbi, "Convolutional codes and their performance in communication systems," IEEE Trans. Communications Technology, vol.COM-19, no.5, pp.751-772, Oct. 1971.

[8] Z. Zhou, M. Kavehrad, and D. Peng, "Indoor positioning algorithm using light-emitting diode visible light communications," Opt. Eng., vol.51(8), July 2012.

[9] M. Nakajima and S. Haruyama, "Indoor navigation system for visually impaired people using visible light communication and compensated geomagnetic sensing," Proc. 1st IEEE International Conference on Communications in China (ICCC), Beijing, China, pp.524-529, Aug. 2012.

[10] S. Arnon, Visible Light Communication, Cambridge University Press, Cambridge, Mar. 2015.

[11] G. D. Forney, "The Viterbi algorithm," Proc. IEEE, vol.61, no.3, pp.268 -278, Mar. 1973.

[12] L. Zeng, D. O'Brien, H. Le-Minh, L. Kyungwoo, J. Daekwang, and O. Yunje, "Improvement of date rate by using equalization in an indoor visible light communication system," Proc. 4th IEEE International Conference on Circuits and Systems for Communications, Shanghai, China, pp.678-682, May 2008.